# Hybrid-Mode Analysis of Multilayered and Multiconductor Transmission Lines

Md. Shah Alam, *Student Member, IEEE*, Masanori Koshiba, *Senior Member, IEEE*, Koichi Hirayama, *Member, IEEE*, and Yoshio Hayashi

***Abstract*—Hybrid-mode propagation properties of multilayered and multiconductor transmission lines are studied by using an efficient vector finite element method (FEM) with high-order hybrid edge/nodal triangular elements, which can give frequency-dependent propagation constants directly. Characteristic impedances are also calculated from the FEM field solutions employing a reciprocity-related definition and taking the modal orthogonality into account. The numerical results of a coupled microstrip line are compared with those of the boundary integral equation technique, and good agreement is obtained. Also, a dual-plane triple microstrip line is analyzed. The approach is found to be very general and able to simultaneously handle different thicknesses and widths of strip conductors. The flexibility of the approach is also shown by including anisotropy in the dielectric substrates of such lines.**

## I. Introduction

RECENT microwave integrated circuits exhibit the use of various complex waveguiding structures having several conductors on various layers of dielectric substrates [1]–[10]. In many cases these transmission lines are asymmetric with equal or unequal strip widths and/or thicknesses [3], [5], [10]. Especially for very small, i.e., micron-sized structures, the conductors are very frequently of unequal widths or thicknesses, even though they apparently look alike with equal widths or thicknesses. Therefore, the multiconductor transmission lines should be handled with great care so that any asymmetry can be accounted for in the analysis. In this context, the finite element method (FEM) is a very flexible and convenient method.

Heretofore, much work have been done to simulate propagation properties of multiconductor transmission lines by using a quasi-TEM approach [2], [7] and spectral domain method (SDM) [1], [3], [5]. Since the microstrip embedded in an inhomogeneous medium supports only hybrid modes, full-wave analyses are required to produce frequency-dependent characteristics. In this regard, the SDM accurately models multiconductor coupled microstrip lines. In the SDM, however, advanced information on the geometry of the problem is required because the Green's function depends on it, and the formulation greatly varies with the structural configuration. The FEM, on the other hand, is very general and does not require any assumptions on the geometry of the problem, except that the problem domain must be finite in extent. Actually, the FEM has also been used to analyze multiconductor structures [6], [9], where full vector magnetic field formulations are employed. In [6] and [9], the triangular elements with second-order Lagrange interpolation polynomials are used together with the penalty function method. Since the nodal elements assign the degrees of freedom to the nodes, they cannot properly model the singularity occurring at the dielectric or metallic edges in the solution domain. Therefore, with this approach, special treatment is required and also the solution accuracy depends on proper choice of the penalty coefficient.

Recently, different approaches with the FEM are being used by many researchers. A revolutionary approach with the hybrid elements [11]–[15], which are comprised of edge and nodal elements has appeared and is leading the simulation of electromagnetics to a new era. With this approach, the edge elements model the transverse field ensuring tangential continuity in the element interfaces and the nodal elements, model the axial fields; thus the approach ensures the true full-wave hybrid-mode analysis, which is essential for modeling any inhomogeneous transmission lines such as microstrip lines and finlines. As the edge elements assign the degrees of freedom to the edges, they allow the field to change its direction abruptly and thus are capable of modeling the fields properly at sharp edges where singularity occurs. Thus, the approach does not need any special treatment of singularities on metal edges.

We have used the FEM approach of [15] to the analysis of lossless and lossy planar transmission lines [16]–[18]. However, the approach has not been applied yet to multilayered and multiconductor transmission lines. In this paper, we have analyzed the propagation characteristics of multilayered and multiconductor transmission lines by using the vector FEM [15]. In the FEM, a generalized eigenvalue equation gives solutions for the phase constants and the transverse fields directly. The field solutions are then further processed to calculate the strip current, modal power, and characteristic impedance.

For a multiconductor transmission line supporting a number of modes, a single value of impedance cannot be defined because there exists a number of paths for currents and different potentials on different strips. There must be different voltages and currents in each conductor for different modes, giving rise to voltage and current matrices, whose size depends on the number of conductors (except the ground conductor) in the transmission line. So, it is necessary to use matrix manipulations and, hence, to produce an impedance matrix.

Manuscript received November 10, 1995; revised October 18, 1996.

M. S. Alam and M. Koshiba are with the Division of Electronics and Information Engineering, Hokkaido University, Sapporo 060 Japan.

K. Hirayama and Y. Hayashi are with the Department of Electrical and Electronic Engineering, Kitami Institute of Technology, Kitami 090 Japan.

Publisher Item Identifier S 0018-9480(97)00824-7.

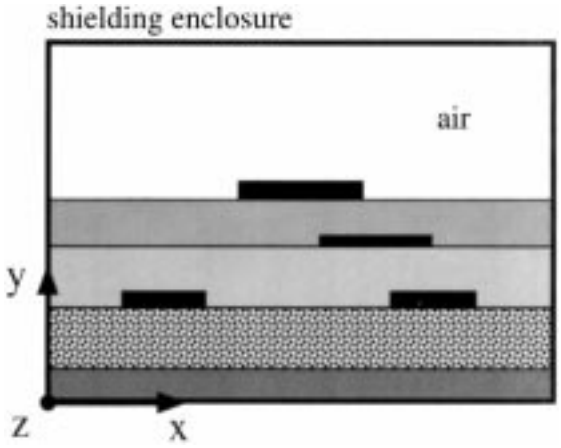


Fig. 1. Cross section of a general multilayered and multiconductor transmission line.

In this paper, we have calculated the total characteristic impedance and the modal characteristic impedance by using some basic matrix manipulations on power and current matrices following the reciprocity-related definition used by [4]. Therefore, we have shown an efficient general procedure using the FEM in conjunction with the reciprocity-based definition of impedance to handle an arbitrary configuration with an arbitrary number of conductors embedded in an arbitrary number of layers. The treatment is very concise and complete and could be useful for many circuit designers in the microwave community. Numerical results are shown for coupled microstrip lines and dual-plane triple microstrip lines. The results are found to be in good agreement with previously published ones.

## II. Statement of the Problem

Fig. 1 shows a general multilayered and multiconductor transmission line. The structure is uniform and infinitely long. There are a number of homogeneous layers in the dielectric materials, which are assumed to be lossless, and isotropic and/or anisotropic. Both the conducting and dielectric regions are assumed to be nonmagnetic. The isotropic material is characterized by relative permittivity $\epsilon_{ri}$, a scalar quantity, and the anisotropic material by the tensor permittivity $[\epsilon_{ri}]$, for the $i$th layer, where

$$[\epsilon_{ri}] = \begin{bmatrix} \epsilon_{rxi} & 0 & 0 \\ 0 & \epsilon_{ryi} & 0 \\ 0 & 0 & \epsilon_{rzi} \end{bmatrix}. \tag{1}$$

The strips are assumed to be perfect conductors with infinite conductivity. These conductors could be very thin or sufficiently thick with different widths and are embedded in different layers, or in the interface between layers. As shown in Fig. 1, $z$ is the propagation direction and for all field components in such a structure, we assume time and longitudinal dependence as $e^{j(\omega t-\beta z)}$ with $\omega$ and $\beta$ being the angular frequency and the phase constant, respectively. There exists as many distinct fundamental modes propagating on the line as the number of conductors located in the shielding enclosure. These modes combine together and form the actual fields around the lines. Each actual mode is decoupled from all other modes and has a different propagation constant. The present work will focus on the study of the modal behaviors of the phase constant and the characteristic impedance.

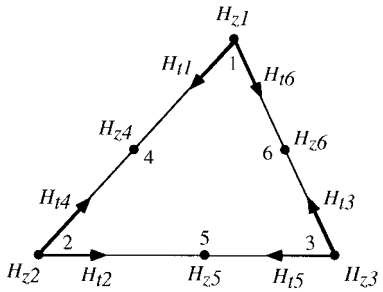


Fig. 2. High-order hybrid edge/nodal triangular element.

## III. Formulation

### A. Finite Element Method

The vector FEM with high-order hybrid edge/nodal triangular elements has been described in detail in [15]. Therefore, for the sake of brevity we will show only the key steps in this paper.

Fig. 2 shows the shape of the high-order hybrid edge/nodal triangular element [15], where we use the magnetic field as the working variable because it will facilitate the computation of current on the strip conductors for each mode, as will be shown in the following sections. The transverse field components in each element are expanded using edge-based interpolation functions

$$\boldsymbol{H}_t = \sum_{i=1}^{6} \boldsymbol{W}_i H_{ti} \tag{2}$$

with

$$\boldsymbol{W}_i = l_{ij} L_i \nabla L_j \tag{3a}$$

$$\boldsymbol{W}_{i+3} = l_{ji} L_j \nabla L_i \tag{3b}$$

where $\boldsymbol{W}_i$ is the edge-based vector shape function, the subscripts $i$ and $j$ always progress modulo 3, $l_{ij}$ is the length of the edge between vertices $i$ and $j$, and $L_i$ is the area coordinate associated with $i$th node. The longitudinal component is expanded using the conventional nodal-based interpolation functions

$$H_z = \sum_{i=1}^{6} N_i H_{zi} \tag{4}$$

where $N_i$ is the nodal-based shape function for $i$th node. The interpolating functions for the shape functions are detailed in [15].

The boundary value problem in the full-wave analysis of an inhomogeneously dielectric-filled waveguide is defined by the

vector wave equation derived from Maxwell's equations

$$\nabla \times ([\epsilon_{ri}]^{-1}\nabla \times \boldsymbol{H}) - k_0^2 \boldsymbol{H} = 0 \quad \text{in} \quad \Omega \tag{5}$$

where $k_0$ is the free space wave number, and $\Omega$ denotes the cross section of the structure whose boundary is composed of perfect electric and/or magnetic walls. The boundary conditions required for the $\boldsymbol{H}$ formulation are homogeneous Dirichlet conditions on perfect magnetic conductors (PMC's) and homogeneous Neumann conditions on perfect electric conductors (PEC's). Thus

$$\boldsymbol{n} \times \boldsymbol{H} = 0 \quad \text{on PMC} \tag{6a}$$

$$\boldsymbol{n} \times ([\epsilon_{ri}]^{-1}\nabla \times \boldsymbol{H}) = 0 \quad \text{on PEC} \tag{6b}$$

where $\boldsymbol{n}$ is the unit vector normal to the surface of the conductors.

Applying the finite element technique to (5) and (6), we obtain a generalized matrix eigenvalue problem

$$[A]\{H_t\} = \beta^2 [B]\{H_t\} \tag{7}$$

where $\{H_t\}$ is the column vector for the edge variables of the whole problem domain which will give the tangential magnetic fields, and $[A]$ and $[B]$ are the finite element matrices and are obtained after some matrix manipulations. The descriptions of their elements are detailed in [15]. The axial fields may also be calculated from the transverse fields [16], [18]. All the FEM field solutions will be employed to produce power and current matrices.

### *B. Characteristic Impedance*

In multiconductor systems with $n$ conductors (except the ground conductor), $n$ fundamental modes which are orthogonal to each other can propagate along the longitudinal direction. Each fundamental mode is specified by its phase constant and the overall power transported along the total conductor configuration. For such a configuration there can be two types of characteristic impedances—the total characteristic impedance and the modal characteristic impedance [4]–[6]. Through the FEM field solutions, the current matrix $[I]$ can be constructed, each element of which is the axial current $I_{ik}$ on $i$th line for a given mode $k$. Thus, for an $n$ conductor system, a complete set of currents will be defined by an $n \times n$ matrix $[I]$. An $n \times n$ voltage matrix $[V]$ can also be constructed with components $V_{ik}$, if modal characteristic impedance $Z_{ik}^m$ is assumed to exist, such that

$$V_{ik} = Z_{ik}^m I_{ik}. \tag{8}$$

Thus, the modal characteristic impedance is defined by the ratio of voltage to current on a line for a given mode. The total characteristic impedance is determined in the matrix form, $[Z^t]$, given by

$$\{V^t\} = [Z^t]\{I^t\} \tag{9}$$

where $\{V^t\}$ and $\{I^t\}$ are arbitrary total voltage vector and total current vector, respectively, due to a superposition of all the modes on each of the $n$ lines. They are obtained from $[V]$ and $[I]$, such that $\{I^t\} = [I]\{A\}$ and $\{V^t\} = [V]\{A\}$. The components $I_i^t$ and $V_i^t$ of $\{I^t\}$ and $\{V^t\}$, respectively, are the total arbitrary current and voltage on $i$th line. The components $A_k$ of $\{A\}$ are the coefficients for mode $k$ in the modal expansion. Therefore, the total characteristic impedance matrix will be given by

$$[Z^t] = [V][I]^{-1} \tag{10}$$

where $[I]^{-1}$ is the inverse matrix of $[I]$. Following the relation $[I]^T[V] = [P]$, the total characteristic impedance matrix becomes

$$[Z^t] = ([I]^T)^{-1}[P][I]^{-1} \tag{11}$$

where $[P]$ is a diagonal matrix and each diagonal element, $P_{kk}$ is the propagating power for the $k$th mode, and $T$ denotes a transpose. Thus, the total characteristic impedance relating the voltage of $i$th line to the current on $j$th line $Z_{ij}^t$ can be calculated from (11), doing some manipulations on matrices $[I]$ and $[P]$. The modal characteristic impedance of the $i$th line for the $k$th mode, $Z_{ik}^m$ can also be easily calculated. The modal characteristic impedance could be useful for studying the nature of hybrid-mode propagation on multiconductor transmission line systems [6]. On the other hand, total characteristic impedance could be useful for the circuit designers, who are always concerned with the equivalent circuits and the characteristic terminations.

### *C. Calculation of Current and Power*

In this subsection, we see how the axial current and the propagating power can be calculated using the FEM field solutions. For evaluating the axial current in $i$th conductor for a given mode $k$, we use Ampere's law as

$$I_{ik} = \oint_{C_i} \boldsymbol{H}_k \cdot d\boldsymbol{l} \tag{12}$$

where the integration contour $C_i$ is taken to be a path around the surface of the $i$th strip. To evaluate the integral, only the tangential fields on the strip surface are required [16].

The propagating power for the orthogonal modes is described by the Poynting vector as

$$P_{kk'}\delta_{kk'} = \iint_{\Omega} [\boldsymbol{E}_k \times (\boldsymbol{H}_{k'})^*] \cdot \boldsymbol{z}\, dx\, dy \tag{13}$$

where $\boldsymbol{E}_k$ is the electric field, the asterisk denotes complex conjugate, and the Kronecker delta $\delta_{kk'} = 0$ if $k \neq k'$ and $\delta_{kk'} = 1$ if $k = k'$. Using Maxwell's equations and the FEM procedure, we can evaluate the power as

$$P_{kk} = \frac{\beta_k}{\omega \epsilon_0} \{H_{tk}\}^\dagger [B]\{H_{tk}\} \tag{14}$$

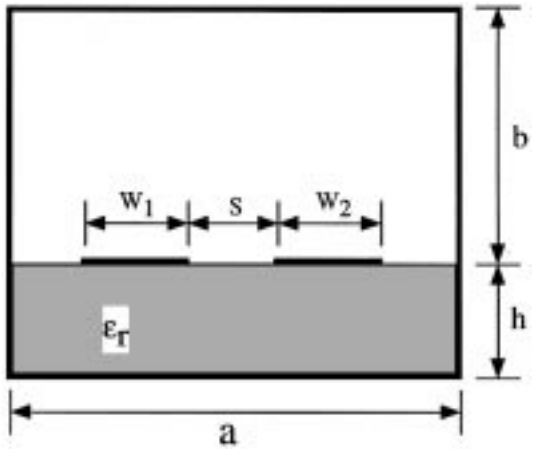


Fig. 3. Cross section of a lossless shielded coupled microstrip line.

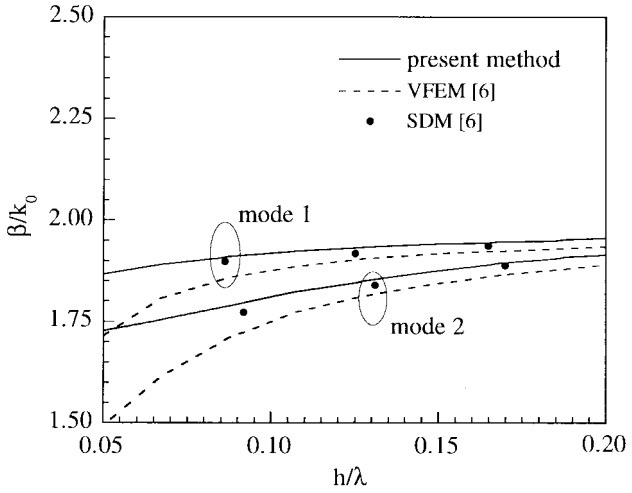


Fig. 4. Normalized propagation constants versus frequency for the coupled microstrip line.

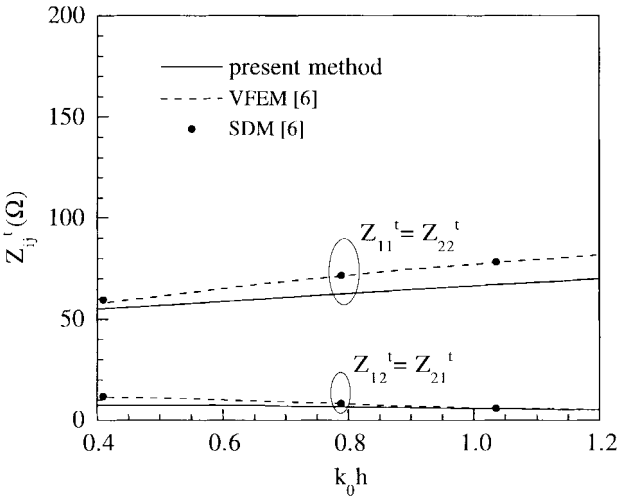


Fig. 5. Total characteristic impedances for the coupled microstrip line.

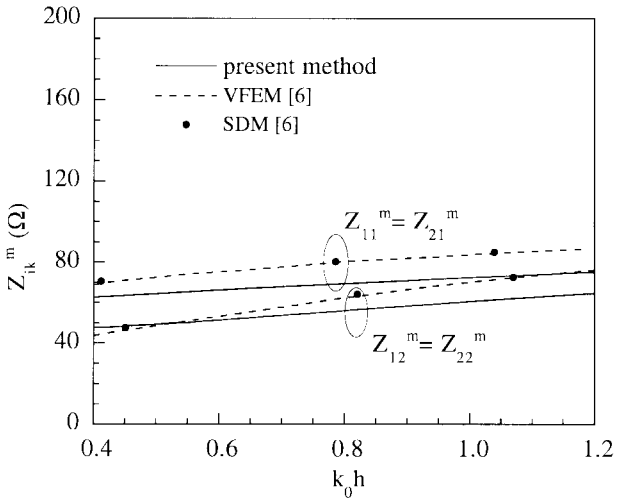


Fig. 6. Modal characteristic impedances for the coupled microstrip line.

where $\epsilon_0$ is the permittivity of free space. The dagger denotes complex conjugate and transpose. Here $[B]$ is exactly the same as that which appeared in the eigenvalue problem (7). Thus, the modal power can be easily calculated using the FEM technique.

## IV. Numerical Results

First, we consider a very simple case of a multiconductor transmission line, i.e., a lossless shielded coupled microstrip line shown in Fig. 3. For the structure, $a = 10$ mm, $h = 1.0$ mm, $b = 4.0$ mm, and the relative permittivity of the substrate, $\epsilon_r = 4.0$. The strips are assumed to be very thin and their widths are $W_1 = W_2 = 2.0$ mm, and the separation between the strips $S = 1.0$ mm. The dispersion curves for the normalized propagation constant is shown in Fig. 4. No assumptions of symmetry is imposed for this structure. The verification is made by comparing our results with those of vector finite element method (VFEM) and SDM reported by [6]. The two modes corresponding to the usual even and odd modes are shown by solid lines, and the results calculated by [6] are shown by dotted lines and circles. We can see that our results are in better agreement with the SDM results than the VFEM results of [6].

Figs. 5 and 6 show the total characteristic impedance and modal characteristic impedance versus frequency, respectively. Even though our results do not agree very well with the results calculated by [6], we can see a like tendency of the curves. From our results we can see that the total characteristic impedance satisfies the reciprocity relation, i.e., $Z_{12}^t = Z_{21}^t$, and also we find that $Z_{11}^t = Z_{22}^t$. The symmetry of $[Z^t]$ is indicative of the reciprocal nature of the transmission lines and the fact that $[Z^t]$ is real is a consequence of the lossless approach to the analysis taken here. It is also found that all modal impedances are positive. Because of the symmetry of the structure, both lines have the same modal impedance $Z_{ik}^m$ for mode $k$; thus, $Z_{11}^m = Z_{21}^m$ (mode 1) and $Z_{12}^m = Z_{22}^m$ (mode 2). The reasons for the discrepancy may be due to the insufficient number of elements in the calculations and/or their results are for the microstrip configuration with strip thickness neglected to zero.

The next example is a dual-plane triple microstrip line shown in Fig. 7. This structure has been analyzed by [8] and [9], where the thickness of the strips are neglected. In our case, we assumed a finite strip thickness, and other parameters

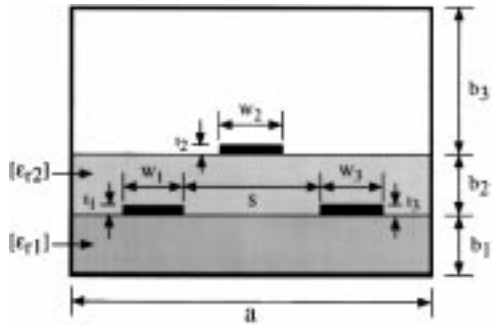


Fig. 7. Cross section of a dual-plane triple microstrip line.

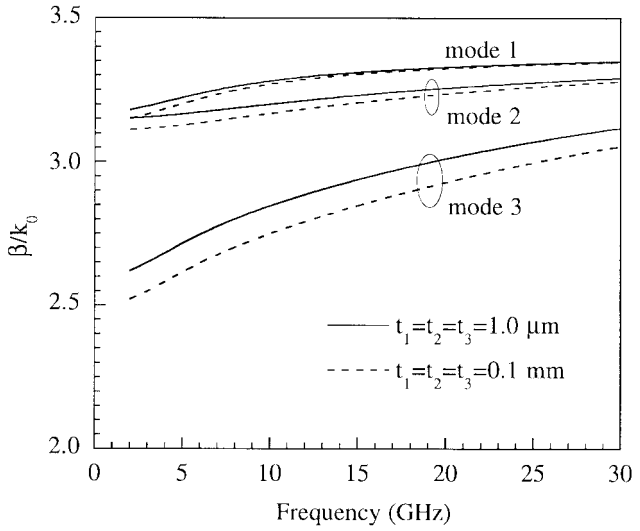


Fig. 8. Normalized propagation constants versus frequency for the dual-plane triple microstrip line.

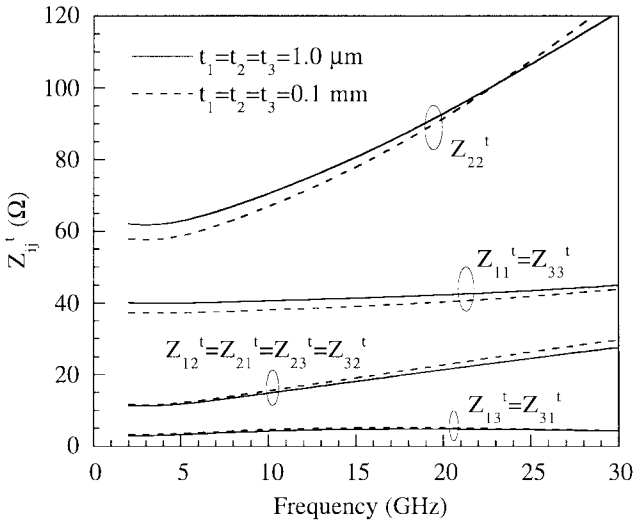


Fig. 9. Total characteristic impedances for the dual-plane triple microstrip line.

are $a = 10.0$ mm, $b_1 = b_2 = 1.0$ mm, $b_3 = 4.0$ mm, the strip widths $W_1 = W_2 = W_3 = 1.0$ mm, and the separation between the strips on the lower plane $S = 2.0$ mm. No assumptions of symmetry are used in this case.

Fig. 8 shows the normalized propagation constant versus frequency for the example of Fig. 7. Three distinct modes

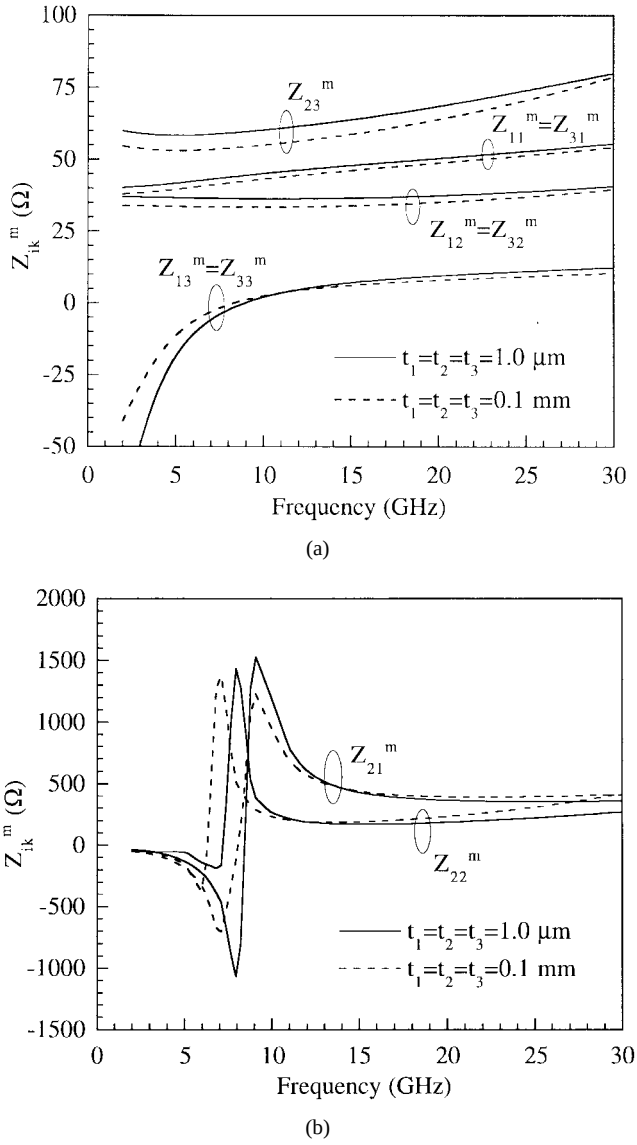


Fig. 10. Modal characteristic impedances for the dual-plane triple microstrip line. (a) $Z_{11}^m, Z_{12}^m, Z_{13}^m, Z_{23}^m, Z_{31}^m, Z_{32}^m$, and $Z_{33}^m$. (b) $Z_{21}^m$ and $Z_{22}^m$.

are shown in the figure, where both layers are anisotropic sapphire substrates with the dielectric permittivity $\epsilon_{rx1} = \epsilon_{rx2} = \epsilon_{rz1} = \epsilon_{rz2} = 9.4$ and $\epsilon_{ry1} = \epsilon_{ry2} = 11.6$. The solid lines with circles and the dashed lines with triangles show the results of two cases: $t_1 = t_2 = t_3 = 1.0$ $\mu$m and $t_1 = t_2 = t_3 = 0.1$ mm, respectively. We can see that thickness affects the propagation constants of mode 1 at lower frequencies, and of modes 2 and 3 over the whole frequency range, where mode 3 is greatly affected. Also, the propagation constants show increasing dispersion behavior with the increase in frequency.

The total characteristic impedances of the dual-plane triple microstrip line are shown in Fig. 9. The numerical results imply that the total characteristic impedance matrix follows symmetric nature as $Z_{11}^t = Z_{33}^t, Z_{12}^t = Z_{23}^t$, and $Z_{21}^t = Z_{32}^t$. Here, we can see that the reciprocity relation, i.e., $Z_{ij}^t = Z_{ji}^t$ is also satisfied. The same symmetry in the impedance matrix has also been assumed in many analyses of three coupled microstrip lines located in the same plane [20], [21].

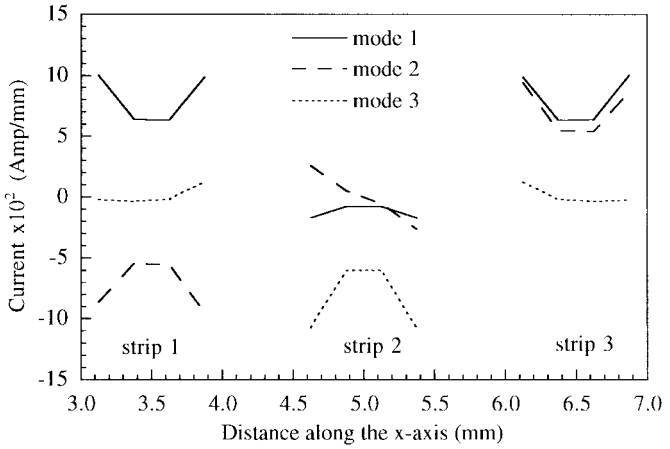


Fig. 11. Current distributions on the bottom surfaces of the three strips of the dual-plane triple microstrip line at 5 GHz.

The modal characteristic impedances are shown in Fig. 10. We have found in the calculations that $Z_{21}^m, Z_{22}^m, Z_{13}^m$, and $Z_{33}^m$ show negative values at certain frequency range (below 10 GHz). For this case, thickness affects the impedance value. Since the modal impedance is nothing but the ratio of voltage to current in one conductor for a given mode, so it could be negative depending on voltage or current of any one if negative. We plotted the longitudinal current distributions along the bottom surfaces of the three strips at 5 GHz and found some negative currents as shown in Fig. 11. As a matter of fact, negative impedances are also reported in [6] and [22].

In the above calculations, we used approximately 350 hybrid edge/nodal triangular elements. The corresponding size of eigenvalue matrix equation follows about 1200 and required memory is about 30 megabytes. Time required to obtain a propagation constant at a given frequency is about 40 min on a NEWS-5000 UA workstation with a speed of 100 MIPS.

From the above numerical results of propagation constants and characteristic impedances, it can be seen that the FEM approach is efficient enough to model multiconductor transmission lines and that the thickness, even if it is very small, should be carefully considered in the analysis. Note, however, that the analysis applies to any nonsymmetric multiple strip configuration as well.

## V. Conclusion

The FEM with high-order hybrid edge/nodal triangular elements has been used for the analysis of general multilayered and multiconductor transmission lines. It has been shown that the FEM approach can be used to generate field solutions for all the modes, which are orthogonal to each other. Propagating power, current flow, and characteristic impedance are also calculated from the FEM field solutions. For multiconductor transmission lines it has been found feasible to calculate two types of characteristic impedances: total characteristic impedance and modal characteristic impedance, where they can be easily produced by using elementary matrix transformations on current and power matrices. Our computation also includes inhomogeneous and anisotropic materials. The approach can be extended to the analysis of more complex structures with stratified media, including bi-isotropic or gyrotropic materials.

## References

[1] T. Kitazawa and Y. Hayashi, "Propagation characteristics of striplines with multilayered anisotropic media," *IEEE Trans. Microwave Theory Tech.*, vol. MTT-31, pp. 429–433, June 1983.

[2] C. Wei, R. F. Harrington, J. R. Mautz, and T. K. Sarkar, "Multiconductor transmission lines in multilayered dielectric media," *IEEE Trans. Microwave Theory Tech.*, vol. MTT-32, pp. 439–450, Apr. 1984.

[3] Y. Fukuoka, Q. Zhang, D. P. Neikirk, and T. Itoh, "Analysis of multilayer interconnection lines for a high-speed digital integrated circuit," *IEEE Trans. Microwave Theory Tech.*, vol. MTT-33, pp. 527–532, June 1985.

[4] L. Wiemer and R. H. Jansen, "Reciprocity related definition of strip characteristic impedance for multiconductor hybrid-mode transmission lines," *Microwave Opt. Technol. Lett.*, vol. 1, pp. 22–25, Mar. 1988.

[5] L. Carin and K. J. Webb, "Characteristic impedance of multilevel, multiconductor hybrid-mode microstrip," *IEEE Trans. Magn.*, vol. 25, pp. 2947–2949, July 1989.

[6] G. W. Slade and K. J. Webb, "Computation of characteristic impedance for multiple microstrip transmission lines using a vector finite element method," *IEEE Trans. Microwave Theory Tech.*, vol. 40, pp. 34–40, Jan. 1992.

[7] J. J. Yang, G. E. Howard, and Y. L. Chow, "A simple technique for calculating the propagation dispersion of multiconductor transmission lines in multilayer dielectric media," *IEEE Trans. Microwave Theory Tech.*, vol. 40, pp. 622–627, Apr. 1992.

[8] C. Seo and C. W. Lee, "Analysis of two-layer three-coupled microstrip lines on anisotropic substrates," *IEEE Trans. Microwave Theory Tech.*, vol. 42, pp. 160–162, Jan. 1994.

[9] C. Seo, "Finite element analysis of two-layer three-coupled microstrip lines on anisotropic substrates," *IEEE Trans. Magn.*, vol. 30, pp. 3112–3115, Sept. 1994.

[10] J. C. Coetzee, "Efficient spectral domain analysis of open asymmetrical multiconductor transmission lines," *Microwave Opt. Technol. Lett.*, vol. 8, no. 4, pp. 206–209, Mar. 1995.

[11] J.-F. Lee, D.-K. Sun, and Z. J. Cendes, "Full-wave analysis of dielectric waveguides using tangential vector finite elements," *IEEE Trans. Microwave Theory Tech.*, vol. 39, pp. 1262–1271, Aug. 1991.

[12] M. Koshiba, *Optical Waveguide Theory by the Finite Element Method*. Tokyo/Dordrecht: KTK Scientific/Kluwer Academic, 1992.

[13] M. Koshiba and K. Inoue, "Simple and efficient finite-element analysis of microwave and optical waveguides," *IEEE Trans. Microwave Theory Tech.*, vol. 40, pp. 371–377, Feb. 1992.

[14] J.-M Jin, *The Finite Element Method in Electromagnetics*. New York: Wiley, 1993.

[15] M. Koshiba, S. Maruyama, and K. Hirayama, "A vector finite element method with the high-order mixed-interpolation-type triangular elements for optical waveguiding problems," *J. Lightwave Technol.*, vol. 12, no. 3, pp. 495–502, Mar. 1994.

[16] M. S. Alam, K. Hirayama, Y. Hayashi, and M. Koshiba, "Analysis of shielded microstrip lines with arbitrary metallization cross section using a vector finite element method," *IEEE Trans. Microwave Theory Tech.*, vol. 42, pp. 2112–2117, Nov. 1994.

[17] M. S. Alam, M. Koshiba, K. Hirayama, and Y. Hayashi, "Vector finite element solution of lossy planar transmission lines," in *1994 Asia Pacific Microwave Conference Proc.*, vol. III, paper no. 32-1, Tokyo, Japan, Dec. 1994, pp. 909–912.

[18] ———, "Analysis of lossy planar transmission lines by using a vector finite element method," *IEEE Trans. Microwave Theory Tech.*, vol. 43, pp. 2466–2471, Oct. 1995.

[19] F. Olyslager, D. De Zutter, and K. Blomme, "Rigorous analysis of the propagation characteristics of general lossless and lossy multiconductor transmission lines in multilayered media," *IEEE Trans. Microwave Theory Tech.*, vol. 41, pp. 79–88, Jan. 1993.

[20] D. Pavlidis and H. L. Hartnagel, "The design and performance of three-line microstrip couplers," *IEEE Trans. Microwave Theory Tech.*, vol. MTT-24, pp. 631–640, Oct. 1976.

[21] V. K. Tripathi, "On the analysis of symmetrical three-line microstrip circuits," *IEEE Trans. Microwave Theory Tech.*, vol. MTT-25, pp. 726–729, Sept. 1977.

[22] A. G. Engel and L. P. B. Katehi, "The effects of finite dielectric layers in multilevel microstrip interconnects," *Int. J. Microwave Millimeter-Wave Comput.-Aided Eng.*, vol. 5, no. 4, pp. 256–263, 1995.

**Md. Shah Alam** (S'94) was born in Serajganj, Bangladesh, in 1966. He received the B.Sc. Eng. degree in electrical and electronic engineering from Bangladesh Institute of Technology, Rajshahi, Bangladesh, in 1989. He received the Japan Government Scholarship for pursuing his graduate studies and received the M.S. degree in electrical and electronic engineering from Kitami Institute of Technology, Kitami, Japan, in 1994. He is presently studying for the Ph.D. degree in electronic engineering at Hokkaido University, Sapporo, Japan.

His interests include the application of the FEM to microwave integrated circuit problems as well as the study of microwave-photonic devices.

Mr. Alam is a Member of the Institute of Electronics, Information and Communication Engineers (IEICE), Japan.

**Masanori Koshiba** (SM'84) was born in Sapporo, Japan, on November 23, 1948. He received the B.S., M.S., and Ph.D. degrees in electronic engineering from Hokkaido University, Sapporo, Japan, in 1971, 1973, and 1976, respectively.

In 1976, he joined the Department of Electronic Engineering, Kitami Institute of Technology, Kitami, Japan. From 1979–1986, he was an Associate Professor of Electronic Engineering at Hokkaido University, and in 1987, he became a Professor there. He has been engaged in research on lightwave technology, surface acoustic waves (SAW), magnetostatic waves (MSW), electron waves, microwave field theory, computer-aided design and engineering for optoelectronic devices, and applications of finite element and boundary element methods to field problems. He has authored or co-authored more than 200 research papers, as well as several books.

Dr. Koshiba is a Member of the Institute of Electronics, Information and Communication Engineers (IEICE), the Institute of Television Engineers of Japan, the Institute of Electrical Engineers of Japan, the Japan Society for Simulation Technology, the Japan Society for Computational Methods in Engineering, and Japan Society of Applied Electromagnetics. In 1987, he was awarded the 1986 Excellent Paper Award by the IEICE.

**Koichi Hirayama** (M'89) was born in Shiranuka, Hokkaido, Japan, on September 8, 1961. He received the B.S., M.S., and Ph.D. degrees in electronic engineering from Hokkaido University, Sapporo, Japan, in 1984, 1986, and 1989, respectively.

In 1989, he joined the Department of Electronic Engineering, Kushiro National College of Technology, Kushiro, Japan. In 1992, he became an Associate Professor of Electronic Engineering at Kitami Institute of Technology, Kitami, Japan. He has been interested in the analysis of propagation and scattering characteristics in electromagnetic and optical waveguides.

Dr. Hirayama is a Member of the Institute of Electronics, Information and Communication Engineers (IEICE) and the Institute of Electrical Engineers of Japan.

**Yoshio Hayashi** was born in Tokyo, Japan, on October 28, 1937. He received the B.E. degree in electrical engineering from Chiba University, Chiba, Japan, in 1961, and the M.E. and D.E. degrees in electronics engineering from Hokkaido University, Sapporo, Japan, in 1965 and 1972, respectively.

From 1961–1969, he served in the Japan Self-Defence Air Force. From 1981–1982 he was a Visiting Scholar of Electrical Engineering at the University of Illinois, Urbana. He is currently a Professor of Electrical and Electronic Engineering at Kitami Institute of Technology, Kitami, Japan. He has been engaged in research on microwave field theory and electromagnetic wave problems.

Dr. Hayashi is a Member of the Institute of Electronics, Information and Communication Engineers (IEICE), Japan.